

See discussions, stats, and author profiles for this publication at: <https://www.researchgate.net/publication/269855980>

The Weighted Longitudinal Profile. A New Method to Evaluate the Longitudinal Evenness of Roads

Article *in* Road Materials and Pavement Design · June 2008

DOI: 10.3166/rmpd.9.135-157

CITATIONS

16

READS

103

2 authors, including:



Andreas Ueckermann

RWTH Aachen University

14 PUBLICATIONS **43** CITATIONS

SEE PROFILE

The weighted longitudinal profile – a new method to evaluate the longitudinal evenness of roads

Andreas Ueckermann – Bernhard Steinauer

*Institute of Road and Traffic Engineering
Technical University of Aachen
Mies-van-der-Rohe-Str. 1
D-52074 Aachen
Germany
ueckermann@isac.rwth-aachen.de
steinauer@isac.rwth-aachen.de*

ABSTRACT. The new method presented in this paper allows the location and individual evaluation of the whole range of phenomena concerned with the longitudinal evenness of road pavements: irregular unevenness, periodicities and transients. It combines the advantages of the response-type methods - implicit valuation of shape and size of unevenness in terms of driving dynamics - with those of purely geometrical methods of evaluation: objectivity and independency of restrictions to certain vibration properties and speeds. The deduction of the method is presented extensively and several example evaluations are given. By comparison to alternative approaches it appears to be a promising evaluation concept.

KEYWORDS: pavement analysis, evenness, longitudinal profile, irregular unevenness, periodic unevenness, transients

1. Introduction

What is the best way to characterize and evaluate the longitudinal evenness of a road? There have been two opposing approaches in the past; one evaluating the dynamic effects of the road on a passenger car or a corresponding measuring device, the other focussing on evaluation of the geometrical properties of the pavement surface. The first approach lacks the requirement of generality because it concentrates on certain dynamic properties; the second is unable to distinguish between the different forms of unevenness - irregular unevenness, periodicities and single (transient) occurrences, unless one uses a whole bunch of individual indicators. The present paper proposes a method which may be able to reconcile the opposing approaches because it is a combination of both.

2. Spectral description of longitudinal unevenness and its limitations

Fig. 1 shows the spectra of five different road surfaces. The ordinate plots the power spectral density (PSD) of the longitudinal elevation profile – a spectral quantity which is proportional to the square of the amplitude of the wavelengths represented in the elevation profile. The abscissa indicates the spatial angular frequency $\Omega=2\pi/\text{wavelength}$ and, below, in the opposite direction, the corresponding wavelength. The wavelengths shown in the graph cover a band of approximately 0.1 to 100 metres.

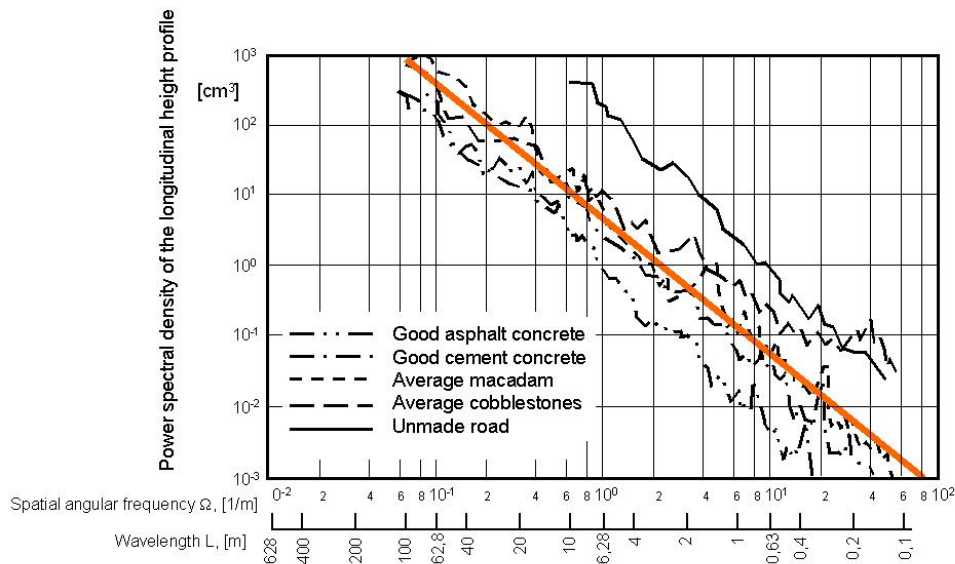


Figure 1. General characteristics of longitudinal evenness, PSD of longitudinal profiles

It is evident from the chart that long waves are associated with high amplitudes and short waves with low amplitudes. Plotted in double logarithmic scale, these power density spectra can approximately be described by a straight line with a gradient between -1.5 and -3. The negative gradient is also referred to as “waviness” (abbreviated: w), while the value of the straight line at a wavelength of 6.28 m (2π m) denotes the “unevenness index” of the road (ISO 8608:1995(E), prEN 13036-5, 2004). In the present context it will be denoted G_0 .

Longitudinal unevenness may be sub-divided into irregular unevenness, periodic unevenness (periodicities) and single (transient) occurrences. The benefit of the PSD approach is that it provides a description of the surface characteristics in terms of two dimensions, wavelength and amplitude. But since it lacks the phase information it is only able to describe the evenness in a statistical manner. The information about location and shape of the unevenness gets lost. Thus, the PSD is best suited for the description of the irregular, overall characteristic of the unevenness.

It is suitable as well for the detection and description of periodic components in the longitudinal profile – but only to a certain extent; if they are too small in amplitude with respect to neighbouring wavebands and/or do not cover a considerable part of the evaluated profile they would not show up in the PSD. Besides that, their power content is distributed over several frequency bands (multiples of the fundamental frequency). The PSD doesn’t say anything about the shape of the periodicity either, which is determinant for the dynamic effects though.

Finally, the PSD approach is unsuitable for the detection and evaluation of transients because the information on both, locality and geometrical shape, gets lost during calculation.

3. Existing approaches to evaluate longitudinal evenness

Existing approaches to the evaluation of longitudinal evenness may roughly be divided in equipment-specific methods and numerical methods based on measured longitudinal elevation profile, see figure 1. Equipment-specific methods include, for example, rolling straightedge, slopometer and profilograph.


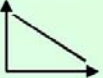


Numerical indices based on measured longitudinal profile			Equipment-specific indices
<p>Geometry</p>  <p>in distance domain (longitudinal profile)</p> <p>Example:</p> <ul style="list-style-type: none"> • standard deviation • maximum values • variance • spatial content • energy content 	<p>Geometry</p>  <p>In spectral domain</p> <p>Example:</p> <ul style="list-style-type: none"> • power spectral density • spectral parameters 	<p>Effects</p>  <p>In distance domain</p> <p>Example:</p> <ul style="list-style-type: none"> • Int. Roughness Index (IRI) • Ride Number (RN) 	<p>Geometry, effects</p>  <p>In distance domain</p> <p>Example:</p> <ul style="list-style-type: none"> • straight edge • profilograph • slopometer • bump integrator

Figure 2. Existing approaches for the evaluation of longitudinal evenness

For monitoring purposes on a net-wide level one prefers to measure the “true” longitudinal elevation profile using a non-contacting profilometer, followed by the calculation of suitable indicators of longitudinal evenness from the measured profile. These can be either “geometrical” indices calculated directly from the elevation profile or its 1st, 2nd (Hudson, 1985, Bruscella, 1999, Rouillard *et al.*, 2000) and even 3rd (Schniering, 1998) derivatives respectively, like e. q. mean, median, standard deviation, root mean square, variance, range, etc., or indices inferred indirectly by means of e. q. wavelet decomposition (Wei *et al.*, 2005, Shirakawa *et al.*, 2005, Kawamura *et al.* 2006) and Fourier transforms (Houbolt, 1962, Braun, 1968, Sayers, 1986, Andr n, 2006). Besides that diverse filtering techniques (moving average, Butterworth, Chebyshev, etc.) are used to pre-process the profile data and to calculate unevenness indices with respect to different wave bands (e.q. short, medium and long waves).

The alternative is to deduce the dynamic response of measuring devices or vehicle components (axles, bodywork, seats, cargo load) and/or the perception of driver/passengers from the measured elevation profile by appropriate filters and to express the output in terms of indicators giving a statistical and/or peak rating for a given evaluation length (response-type indicators). Approaches of this kind include, amongst others, the International Roughness Index, IRI (Sayers *et al.*, 1986, Sayers, 1996), the Half-Car Roughness Index, HRI (Sayers, 1989), even a Full-Car Roughness Index (Capuruc o *et al.* 2005) and the Ride Number, RN (ASTM E 1489-98), which is defined as an exponential transform of the Profile Index (PI). The Profile Index, in turn, uses the same quarter car filter as the IRI, but with other coefficients. The Ride Number is a “comfort” number, scaled from 5 (perfectly smooth) to 0 (maximum possible roughness) and based on human rating experiments.

A more recent approach of human rating experiments uses fuzzy set theory (Loizos, 2001). The results were compared to IRI measurements. Another example of a response-type indicator is the dimensionless “Dynamic Evenness Index”, LWI (Ueckermann, 2002). The LWI uses 3 different vehicle filters along with a “human perception” filter (acc. to ISO 2631-1:1997) and incorporates the effects of longitudinal unevenness on comfort, driving safety, pavement loading and loading of freight cargoes, the greatest of them within an evaluation section being determinant for the LWI.

One of the drawbacks of response-type indicators as compared to geometrical indicators is that they are linked to specific speeds and system properties, so that evaluation may not be sufficiently comprehensive or objective. It can, however, be argued that the point of interest for evaluation is not the geometrical shape of the road surface, but its dynamic effects. The advantage of the response type indicators is that they permit differentiated evaluation of longitudinal evenness with respect to irregular, periodic and local characteristics.

Some of the above mentioned evaluation approaches are used in a more academic environment, others are widely used in pavement monitoring practice on a national or even international level. Diverse national and international experiments have been conducted in the past in order to correlate and harmonize evenness measuring and evaluation methods, like the International Road Roughness Experiment, IRRE, (Sayers *et al.*, 1986), the European FILTER experiment (Alonso *et al.*, 2001) and the PIARC EVEN experiment (Schmidt, 2001). A recent comparison between Profile Index, PI, and International Roughness Index, IRI, can be found in Wilde *et al.* (2007). For a comparison of three widely used evenness evaluation methods in Europe, IRI, PSD and Wave Bands Analysis, see Delanne *et al.* (2001). A rather comprehensive table of roughness devices and indicators has been put together by Pratico (2004) and Boscaino *et al.* (2004).

The method presented in this paper is intended for road maintenance and acceptance inspection purposes. It is able to reconcile the above mentioned two opposing approaches because it uses features of both. Along with the deduction of the method let us first think about suitable limiting values for the longitudinal unevenness.

4. Limiting values for longitudinal evenness

The specific question that arises with the evaluation of unevenness is what thresholds should be set with respect to the different lengths and forms of unevenness. This involves the definition of limiting curves for the longitudinal unevenness. In the context of PSD analysis a standard specifies how to define limiting values and classes for road pavements and airfields (ISO 8608:1995(E)). A corresponding empiric background for PSD roughness evaluations exists in Germany, for example, for about 15 years through net-wide pavement monitoring.

For road maintenance and acceptance inspection purposes different unevenness limits (levels) have been defined, such as target value, acceptance value, warning value and threshold value (Buehler *et al.*, 2002). The target value corresponds to the desired value for a newly-constructed roadway. The acceptance value marks the minimum requirement for a newly-constructed roadway. The warning value describes a road condition which should trigger intensive observation, analysis of the causes of the poor state of the road surface and possibly the planning of suitable measures. Finally, the threshold value describes a condition that should implement constructional or traffic-restricting actions.

For long-distance highways, limiting values for G_0 of 1, 3 and 9 cm^3 have been specified for the target, warning and threshold values respectively, along with a waviness of $w=2$. They mark a set of 3 straight lines in a log-log PSD plot similar to that line shown in Fig. 1, which likewise exhibits a waviness (i.e. a negative gradient) of about 2, but differ in the unevenness coefficient G_0 . The implied limiting curves obey the relationship:

$$G(\Omega) = G_0 \cdot \left(\frac{\Omega}{\Omega_0} \right)^{-2} \quad [1]$$

where Ω_0 denotes the spatial angular frequency for the reference wavelength of 6.28 m (2π m), and is referred to as the reference frequency. It has a value of $\Omega_0 = 2\pi/(2\pi \text{ m}) = 1 \text{ m}^{-1}$.

The following remarks serve solely to explain how the limiting curves in terms of spectral densities, $G(\Omega)$, can be transformed into limiting curves of the form $H(L)$, i.e. in the form of height-wavelength relationships.

Fig. 3 exemplifies the desired height-wavelength relationship for the target value, a function that still has to be deduced. The figure also depicts those wavelength bands in which the axle, the passengers and the bodywork react most sensitively at a speed of 40 km/h; they are 1-2 m for the axle, 2-4 m for the passengers (comfort) and 4-8 m for the bodywork. It is apparent that the resonance bands merge with one another (an intentional feature in vehicle design) and that their width can be described by means of octaves.

If the speed of the vehicle is doubled to 80 km/h, the relevant bands shift to 2-4, 4-8 and 8-16 m respectively and hence to greater unevenness. If the speed is halved, on the other hand, the wavelength band is likewise halved and the excitation is characterized by smaller unevenness levels.

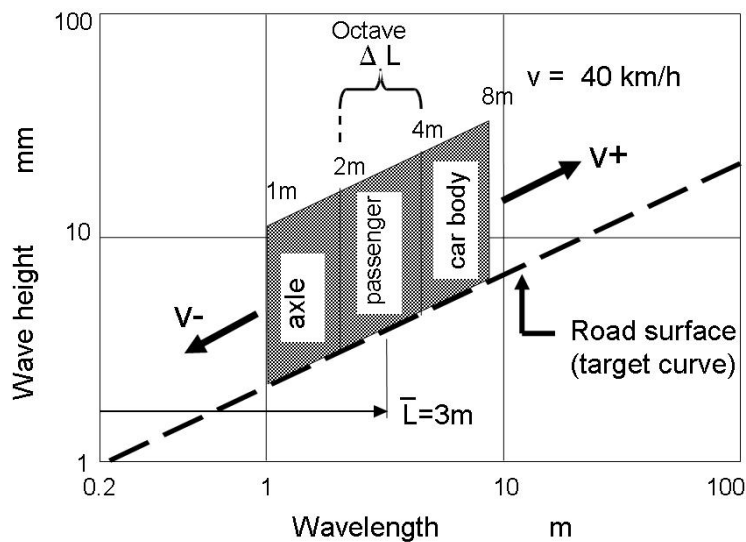


Figure 3. Deducing the limiting values for the longitudinal evenness

This leads us to the deduction of the limiting curves presented above:

The variance (the square of the standard deviation) of the longitudinal elevation profile is equivalent to the integral of the respective spectral density, no matter whether the PSD is expressed as a function of the frequency, Ω , or the wavelength, L . We can write:

$$\sigma^2 = \int_0^\infty G(\Omega) d\Omega = \int_0^\infty G(L) dL \quad [2]$$

with $G(\Omega)$ and $G(L)$ being the power spectral density of the profile, expressed as a function of the spatial angular frequency, $\Omega=2\pi/L$, and as a function of the wavelength, L , respectively. From eq. [2] follows with $L=2\pi/\Omega$:

$$G(L) = \frac{d\Omega}{dL} G(\Omega) = \frac{\Omega^2}{2\pi} G(\Omega) \quad [3]$$

With [1], i.e. for an “average” irregular road with a waviness $w=2$, this yields:

$$G(L) = \frac{\Omega^2}{2\pi} \cdot G_0 \cdot \frac{\Omega^{-2}}{\Omega_0^{-2}} = \frac{\Omega_0^2}{2\pi} \cdot G_0 \quad [4]$$

Filtered by a band-pass filter with band width ΔL centered at \bar{L} we can write by analogy with [2] and using eq. [4]:

$$\sigma_{\Delta L} = \sqrt{\int_{\bar{L}-\Delta L/2}^{\bar{L}+\Delta L/2} G(L) dL} = \sqrt{G(\bar{L}) \cdot \Delta L} = \sqrt{\frac{\Omega_0^2}{2\pi} G_0 \cdot \Delta L} \quad [5]$$

We have stated above that the sensitivity bands of axle, driver and bodywork can be considered roughly as octave bands. For octaves, it is true that:

$$\frac{\Delta L}{\bar{L}} = \frac{2}{3} \quad [6]$$

yielding the following expression for the octave-related standard deviation of the longitudinal evenness ([5] and [6]):

$$\sigma_{oct}(\bar{L}) = \sqrt{\frac{\Omega_0^2}{2\pi} G_0 \cdot \frac{2}{3} \cdot \bar{L}} = \sqrt{\frac{\Omega_0^2}{3\pi} G_0 \cdot \bar{L}} \quad [7]$$

Continuing to assume a normal distribution for the octave-band filtered profile, we can state that 99.9 % of the data are within a range of $\pm (3.29 \cdot \sigma_{oct})$ around the mean value.

This leads us to formulation of the maximum octave-related height (=range) of the longitudinal unevenness:

$$H(\bar{L}) = 2 \cdot 3.29 \cdot \sqrt{\frac{\Omega_0^2}{3\pi} G_0 \cdot \bar{L}} \quad [8]$$

Equation [8] describes the limiting curves we were looking for.

Setting G_0 to 1, 3 and 9 cm^3 , we obtain the 3 limiting functions (Fig. 4) as a function of the centre wavelength. The figure indicates that, for example, the unevenness height in an octave band around 30m, i.e. from 20 to 40m, may not exceed a total of 12 mm in order to comply with the target value.

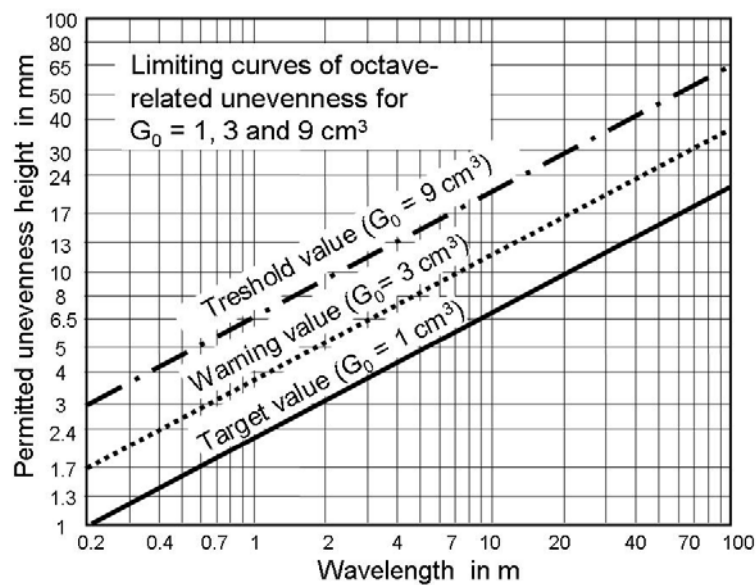


Figure 4. Limiting values of octave-band related longitudinal unevenness

The formulae of the limiting curves shown in Fig. 4 are summarized in Table 1.

Permitted unevenness height (=range)	target value ($G_0 = 1 \text{ cm}^3$)	warning value ($G_0 = 3 \text{ cm}^3$)	threshold value ($G_0 = 9 \text{ cm}^3$)
$H \text{ [mm]}$	$2.2 \cdot \sqrt{L/[m]}$	$3.8 \cdot \sqrt{L/[m]}$	$6.6 \cdot \sqrt{L/[m]}$

Table 1. Limiting curves of octave-band related longitudinal unevenness

5. The Weighted Longitudinal Profile (WLP)

The method described in this paper evaluates the longitudinal road profile with respect to the limiting curves given in Fig. 4. In essence, this is a matter of transforming the wavelength-dependent (spectral) presentation and evaluation according to Fig. 4 into an equivalent distance-dependent presentation evaluated according to Fig. 5. The transformation is performed by means of a “weighting function“, which will be deduced in Section 6.

The calculation scheme essentially consists of three steps: 1) filtering of the measured raw profile to wavelengths of less than 100 m, 2) weighting of the pre-filtered profile and 3) calculation of the standard deviation and the range of variation of the weighted profile. These three steps are illustrated on the right-hand side of Fig. 6. The middle part of the figure indicates the influence of the respective steps on the longitudinal profile. Finally, the left-hand side of the figure depicts the respective steps in the spectral domain. The next chapter is concerned with the deduction of the weighting function.

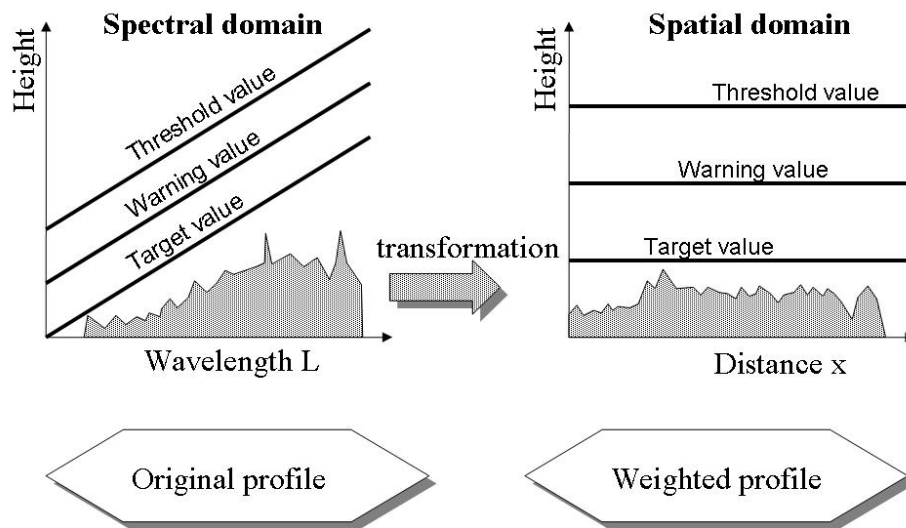


Figure 5. *Transfer of the limiting function from spectral to spatial domain*

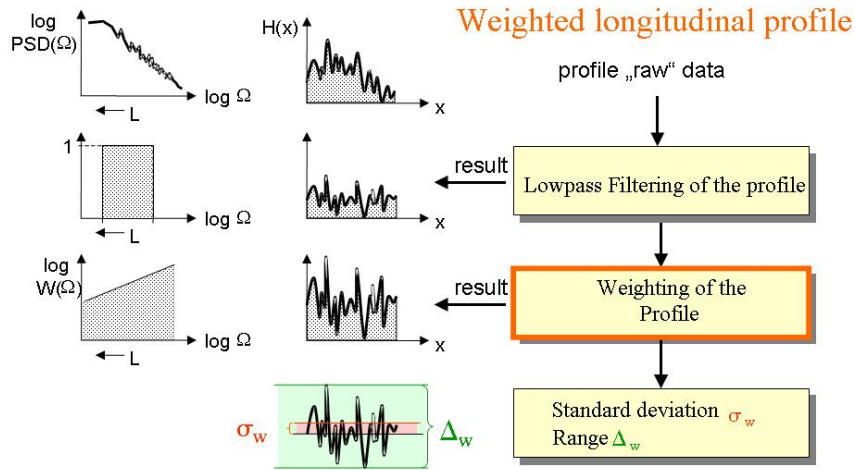


Figure 6. The Weighted Longitudinal Profile – calculation steps (right-hand-side of the figure)

6. Deduction of the weighting function

For the deduction of the weighting function we recall equation [8] which is the equation that describes the limiting function in the spectral domain:

$$H(L) = 2 \cdot 3.29 \cdot \sqrt{\frac{\Omega_0^2}{3\pi} G_0 \cdot L} \quad [8]$$

(Note: Equation [8] is plotted in fig. 4 for 3 different limiting values of G_0).

In the following a transfer function shall be deduced which is able to transform the limiting functions according to eq. [8] into the spatial domain as shown in fig. 5.

For this purpose we recall equation [5] and consider an unfiltered profile containing the whole range of relevant wavelengths from 0.2 to 102.4 m. In that case ΔL in eq. [5] becomes: $\Delta L = \Delta L_{tot} = 102.2$ m.

If we, like before, assume a normal distribution for the profile, we can determine the range of variation by:

$$H_{tot} = 2 \cdot 3.29 \cdot \sigma_{tot} = 2 \cdot 3.29 \cdot \sqrt{\frac{\Omega_0^2}{2\pi} G_0 \cdot \Delta L_{tot}} \quad [9]$$

Equation [9] is the description of the limiting function in the spatial domain.

Now, let us formulate the transformation of the spectral domain into the spatial domain as follows:

$$H(L) \cdot W(L) = H_{tot} \quad [10]$$

For the transformation function $W(L)$ – referred to below as the weighting function – it follows from [8] and [9] that:

$$\underline{\underline{W(L) = \frac{H_{tot}}{H(L)} = \frac{2 \cdot 3.29 \cdot \sqrt{\frac{\Omega_0^2}{2\pi} G_0 \cdot \Delta L_{tot}}}{2 \cdot 3.29 \cdot \sqrt{\frac{\Omega_0^2}{3\pi} G_0 \cdot L}} = \sqrt{\frac{3\Delta L_{tot}}{2L}} = 12.4 \cdot L^{-0.5}}} \quad [11a]$$

or

$$W(\Omega) = 12.4 \cdot \frac{\sqrt{2\pi}}{\sqrt{2\pi}} \cdot L^{-0.5} = \frac{12.4}{\sqrt{2\pi}} \cdot \sqrt{\Omega} = 4.95 \cdot \sqrt{\Omega} \quad [11b]$$

Fig. 7 presents the weighting function as a function of the reciprocal of the wavelength, the wave number or repetency, $n=1/L$.

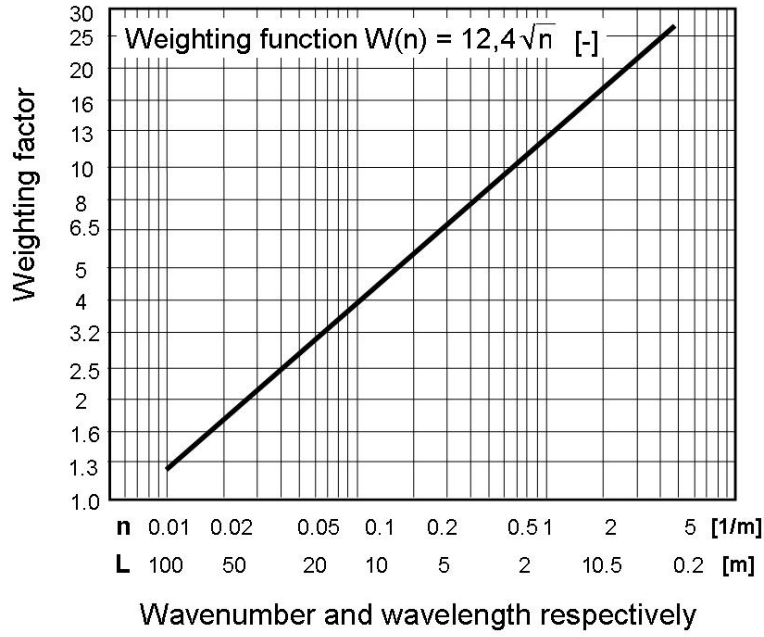


Figure 7. Weighting function as a function of wave length and wave number

7. The evaluation method in detail

Before we look at some sample applications it is necessary to examine the question: What happens to the (octave-band related) limiting functions shown in Fig. 4 when they are multiplied by the weighting function? Do they become “horizontal” limiting values as intended and shown in figure 5?

According to equation [7], the standard deviations of these limiting curves are:

$$\sigma_{oct}(\bar{L}) = \sqrt{\frac{\Omega_0^2}{3\pi} G_0 \cdot \bar{L}} \quad [12]$$

with \bar{L} being the mean wavelength of the octave and G_0 the spectral limiting value.

According to equation [11a], the weighting function is:

$$W(\bar{L}) = \sqrt{\frac{3\Delta L_{tot}}{2\bar{L}}} \quad [13]$$

So, if we multiply the limiting functions, eq. [12], by the weighting function, eq. [13], this results in the following expression:

$$\sigma_{oct,w} = \sqrt{\frac{\Omega_0^2}{2\pi} G_0 \cdot \Delta L_{tot}} = \sigma_{\Delta L,tot} \quad [14]$$

Equation [14] states that the weighting procedure “lifts” each of the (in total) 9 octaves of the limiting curves to the same standard deviation and hence to the same power content, which equals exactly the power content of the original profile, $\sigma_{\Delta L,tot}$, see equation [9]. This means firstly, that the weighting procedure leads to a limiting function of constant level, which was to be proved, and secondly, that the power content of the limiting function for the *weighted* longitudinal profile is 9 times the power content of the limiting function for the *original* profile.

In order to take this into account, the weighting procedure is designed such that the power of the limiting curves of the *weighted* profile is reduced again to one ninth, i.e. to the power content of the limiting curves for the *original* profile. This leads to the calculation scheme shown in figure 8 which is the final calculation scheme for the *weighted* longitudinal profile. The weighting factors shown in Fig. 8 allow for this reduction.

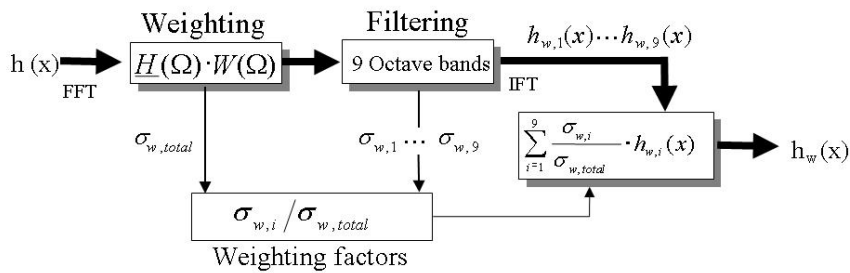


Figure 8. Calculation scheme for the Weighted Longitudinal Profile

Fig. 8 shows the method of evaluation in detail: the longitudinal profile, $h(x)$, limited to a maximum wavelength of 102.4 m, is first converted by Fourier transformation into a spectrum $\underline{H}(\Omega)$, and then multiplied by the evaluation function $W(\Omega)$. The resulting spectrum is now divided into a total of 9 octaves, and each octave is inverse transformed into the spatial domain. This yields nine octave-band-filtered weighted sub-profiles $h_{w,i}(x)$, the weighted sum of which gives the *weighted* longitudinal profile. The 9 weighting factors are obtained from the ratio of the standard deviation of the sub-profiles, $\sigma_{w,i}$, to the standard deviation $\sigma_{w,total}$ of the *sum* of the weighted sub-profiles.

Let's clarify the procedure by means of another figure; it is apparent from Fig. 9 that, following the Fourier transformation (FFT) and multiplication by the weighting function, the inverse transformation into the spatial domain (IFT) is performed solely in relation to the octaves, i.e. for a total of nine neighbouring wavebands "i". This results in 9 sub-profiles $h_{w,i}$, whose weighted sum represents the weighted longitudinal profile. The numerator of the 9 weighting factors is the standard deviation of the respective sub-profiles, $\sigma_{w,i}$. The denominator is the standard deviation of the sum of the 9 sub-profiles, $\sigma_{w,total}$.

The weighting factors ensure that each of the 9 sub-profiles is included in the weighted longitudinal profile in accordance to its contribution to the total power.

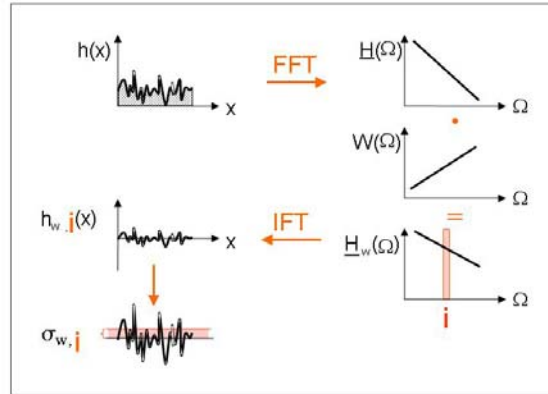


Figure 9. Octave-related evaluation of longitudinal unevenness

The reason for performing the inverse transformation with respect to the octaves, and not in a single step for the entire spectrum, lies in the circumstance already indicated above, that the vehicle axle, the bodywork and the passengers have wavelength-sensitive bands (resonance bands) lying in successive octave ranges. *The chosen procedure enables the evaluation method to take account of, for example, pronounced periodicities (narrow-band spectral sub-components with comparatively high power content) in accordance with their contribution to the total power and hence in accordance with their relevance for driving dynamics.*

8. Limiting values for the Weighted Longitudinal Profile

As shown in Fig. 6, the standard deviation and range of the weighted longitudinal profile are used as indicators for the evenness. The respective target, warning and threshold values can be determined using eq. [9] since the calculation scheme of the weighted longitudinal profile ensures (as just has been explained) that the limiting values for the *weighted* profile are the same as those for the *original* profile. They are based on a maximum wavelength of 102.4 meters and are given in Table 2. The indicator Δ_w corresponds to H_{tot} and σ_w corresponds to σ_{tot} in eq.[9].

Indicator	Target value ($G_0 = 1 \text{ cm}^3$)	Warning value ($G_0 = 3 \text{ cm}^3$)	Threshold value ($G_0 = 9 \text{ cm}^3$)
$\sigma_w [\text{mm}]$	4.5	7.5	12.5
$\Delta_w [\text{mm}]$	28	48	82

Table 2. Limiting values for the weighted longitudinal profile acc. to equation [9] (values slightly rounded up)

9. Exemplary application to irregular, periodic and transient unevenness

Fig. 10 shows a road of irregular longitudinal unevenness, for which $G_0 = 1 \text{ cm}^3$ and $w = 2$. This road corresponds to our “target value” road, possessing the height-wavelength characteristics of the target value limiting curve (see Fig. 4).

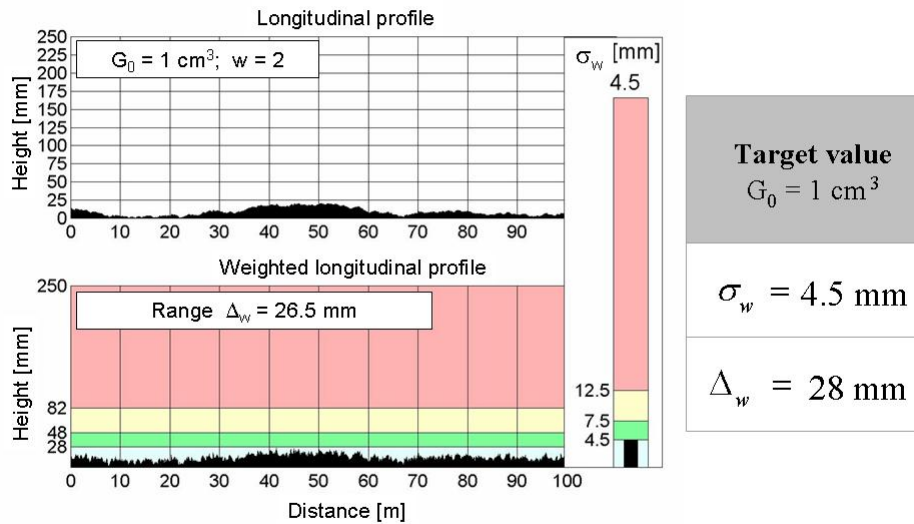


Figure 10. Good road with irregular unevenness, $G_0 = 1 \text{ cm}^3$, $w = 2$.

The top half of the figure shows the original longitudinal profile, the bottom half the weighted longitudinal profile. As expected, the range of the weighted longitudinal profile, 26.5 mm, is at the level of the target value (28 mm). The same is true of the standard deviation, which is shown in the bar chart (to the right of the longitudinal profiles). At 4.5 mm, this coincides exactly with the target value.

Fig. 11 shows a road with irregular unevenness attaining the threshold value ($G_0 = 9.2 \text{ cm}^3$, $w = 2$). The weighted longitudinal profile yields a range of 81.3 mm (just below the threshold value, see table 2) and a standard deviation of 12.8 mm (just above the threshold value – see bar chart).

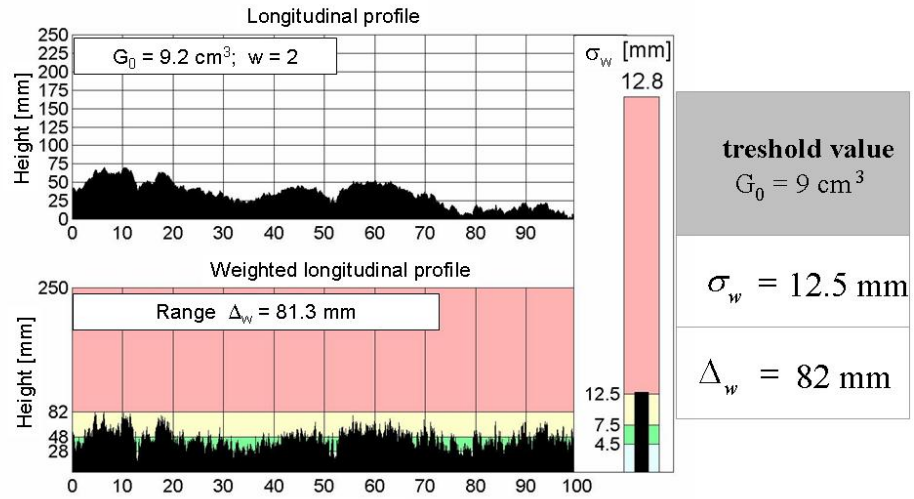


Figure 11. Poor road with irregular unevenness, $G_0 = 9.2 \text{ cm}^3$, $w = 2$.

It is evident from these two examples that the irregular unevenness can be evaluated very effectively using the weighted longitudinal profile, and that the deduced limiting values are appropriate.

Fig. 12 shows a periodicity (“washboard surface”) with a length of 5.5 m and a height of 15 mm (top half of the figure). According to Fig. 4 or Table 1, 15 mm is the threshold value for this wavelength. The weighted longitudinal profile (bottom half of the figure) confirms this, with a range of 83.4 mm (just above the threshold value). However, the standard deviation of the weighted longitudinal profile (28 mm, see the bar chart to the right) extends well into the red zone, exceeding the threshold by more than twice its value. This is due to the fact that the limiting values for the standard deviation rest on the assumption of an irregular normally-distributed roughness characteristic. In this case, however, we are concerned with a harmonic wave, which is known to have a much higher standard deviation than an irregular

normally-distributed characteristic of the same total height (the precise factor is: $3.29/\sqrt{2} = 2.3$, corresponding fairly accurately to the ratio 28/12.5).

Fig. 13 shows a 20 m periodicity with heights around 30 mm (top half of the figure). According to Fig. 4 or Table 1, a height of 30 mm meets the threshold value for this wavelength. The weighted longitudinal profile (bottom half of the figure) likewise fluctuates around the threshold value, confirming that the weighted longitudinal profile is highly suitable for evaluating periodic unevenness.

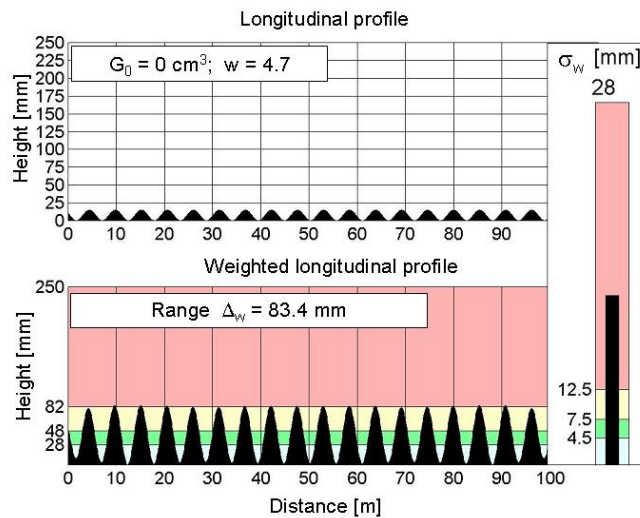


Figure 12. Periodicity (Length: 5.5 m, Height 15.5 mm).

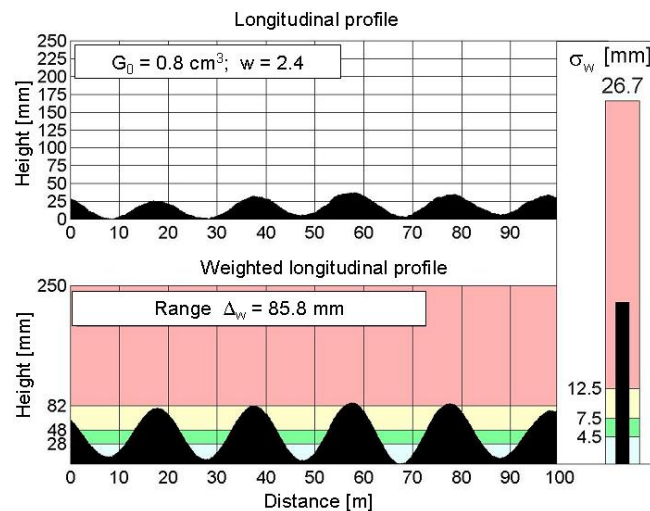


Figure 13. Periodicity (Length: 20 m, Height about 30 mm).

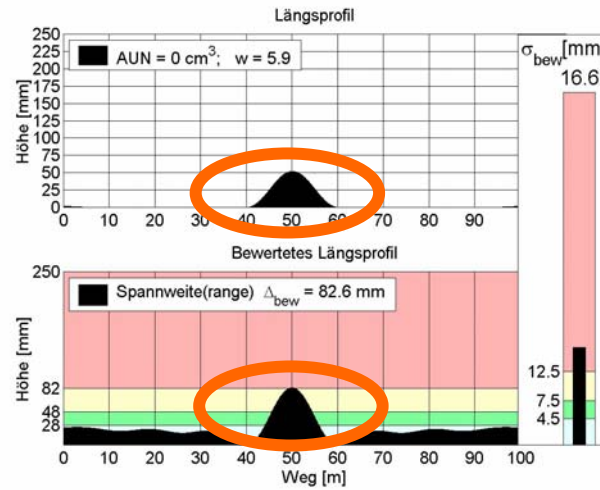


Figure 14. Single bump (Length: 20 m, height about 50 mm).

Fig. 14 shows an unevenness of the same shape and the same length (20 m) as Fig. 13 but in terms of a single bump. Note that the height for the single bump is allowed to be 52 mm to meet the threshold value as opposed to 30 mm for the periodic bump (Fig. 13), which corresponds fairly accurately to a factor of $\sqrt{3}$. This is roughly the factor which can also be found from dynamical analyses in Mitschke *et al.* (1986), where the influence of single and periodical components of unevenness on comfort and vehicle dynamics was examined. This indicates that the evaluation method presented here is able to distinguish satisfactorily between single and periodic unevenness, placing lower limiting values on periodicities because of their ability to cause resonances at certain velocities.

Finally, Fig. 15 shows the (partly saw-toothed) longitudinal profile of a bad concrete pavement (top half of the figure). The weighted longitudinal profile (bottom half) yields, due to the octave-band filtering, a much more realistic picture of the pavement condition than the unevenness coefficient, G_0 , which suggests the pavement to be in a much better condition (just above the warning value of 3 cm³).

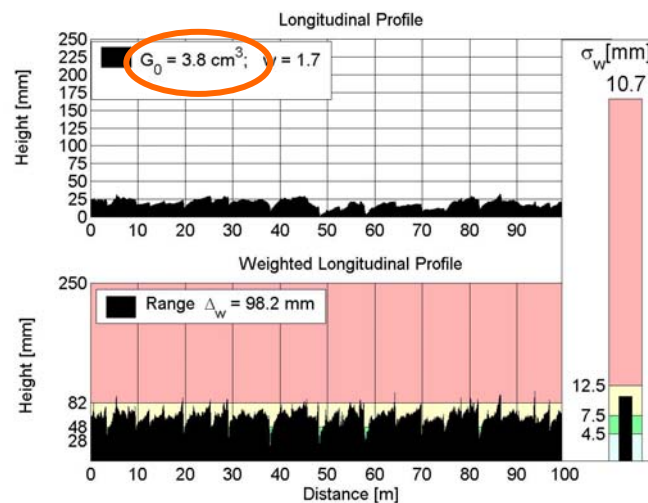


Figure 15. bad concrete pavement

These examples may suffice to demonstrate the suitability of the method for evaluating the longitudinal evenness in terms of irregular, periodic and transient unevenness.

10. Experiences with the Weighted Longitudinal Profile

In recent years the Weighted Longitudinal Profile has been intensely tested. Through different campaigns of net-wide road monitoring it has been applied successfully to the whole highway network in Germany and is intended to become a standard for road maintenance and acceptance inspection purposes. The method proved to be a suitable indicator for the longitudinal evenness on a net-wide level, as well as an appropriate input parameter for pavement management purposes. The ability to detect locations of deficient evenness and to individually rate according to the irregular, periodic and transient nature of the unevenness could be verified. Results have been compared to subjective ratings by a team of experts and good agreement could have been found, both, in terms of locality and rating of the unevenness. The new method proved to be superior to the method in use, the PSD method, insofar that transient and periodic occurrences for the first time became “visible” and assessable to the evaluation of evenness. For testing and demonstration purposes some evaluations have been made recently for authorities in Austria, the Netherlands, Spain, Great Britain and France. An example evaluation is given in figures 16 and 17.

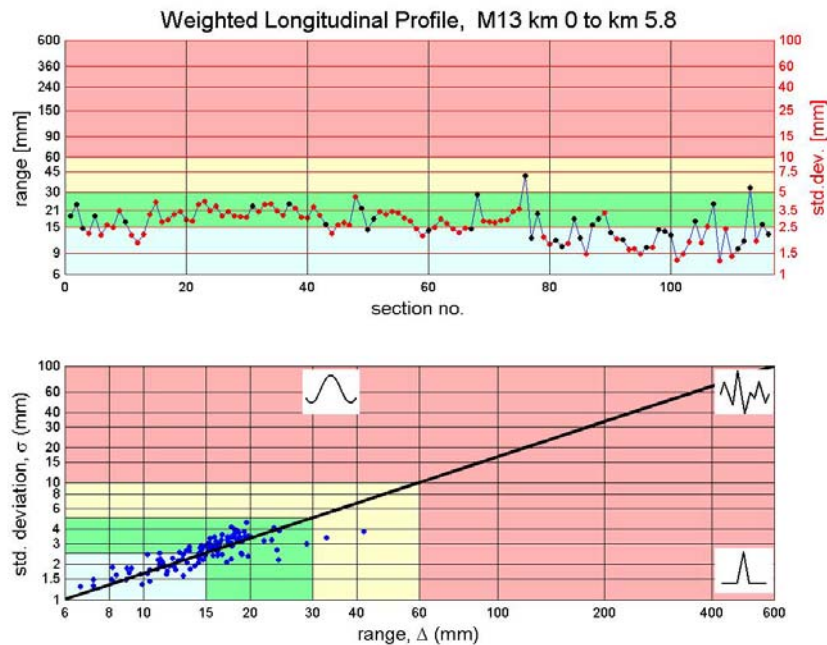


Figure 16. road, 5.8 km long, with evenness mostly between target and warning level (green coloured area, see upper graph)

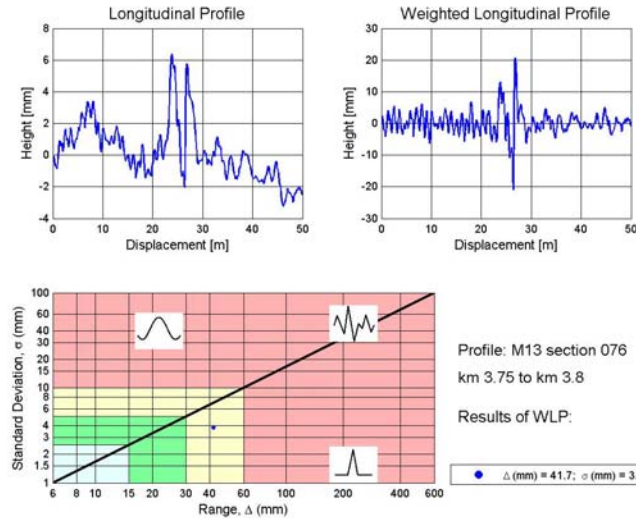


Figure 17. detail of the road shown in figure 16: section 76 (the section with the highest unevenness – above the warning level, yellow marked area)

Figure 16 shows the evaluation result for a 5.8 km long part of a road with unevenness mainly between target and warning value (green coloured area), especially in the first 80 sections. The sections above section 80 are more even in average. The upper graph in figure 16 shows the ratings along the road. A black dot means that the *range* was decisive for the rating of that very section and the scale to the left applies. Likewise, a red dot means that the *standard deviation* was decisive for the rating of that very section and the scale to the right of the graph applies.

The lower graph in figure 16 shows the results of every section in terms of the 2 indicators, standard deviation and range of variation. Only 2 of the 116 sections are above the warning level, see yellow coloured area. Dots considerable below the diagonal imply that the respective sections are dominated by a transient character, while dots considerable above the diagonal indicate that the respective sections have a “wavy” and potentially periodic character. Dots “along” the diagonal, however, are an indication of an irregular character.

Figure 17 lets us take a closer look to the section with the worst unevenness, which is section 76. The lower graph in figure 17 conforms to the lower graph in figure 16 which we just explained. The upper part exhibits 2 graphs, the original (measured) profile on the left and the Weighted Longitudinal Profile on the right-hand side. The transient can be found right in the middle of the section. Here we can see one feature of the Weighted Longitudinal Profile: it amplifies transients, brings them out of their surrounding environment; compare the height of the transient in the WLP with that one in the original profile; we find an amplification factor of $40/8 = 5$. The part before the transient exhibits a periodicity with a wavelength of about 1.2 meters, whereas the part behind the transient exhibits a rather irregular character. Decisive for the rating of this particular section is the transient though.

Further obvious examples of transients and periodicities are given in figures 18 and 19 respectively. Note that the WLP enhances the dominating effects of the particular sections. The transient of very short duration has got a height of about 10 mm and is rated to be above the threshold value, which means it should be repaired. The periodicity has got an amplitude of 3 mm and is rated to be above the warning value and far from being accepted, if the section would have been newly paved. As you can see, the limits are set quite restrictive, but in accordance to the dynamic effects. Of course the limiting values can be changed according to the particular needs of the road management authorities.

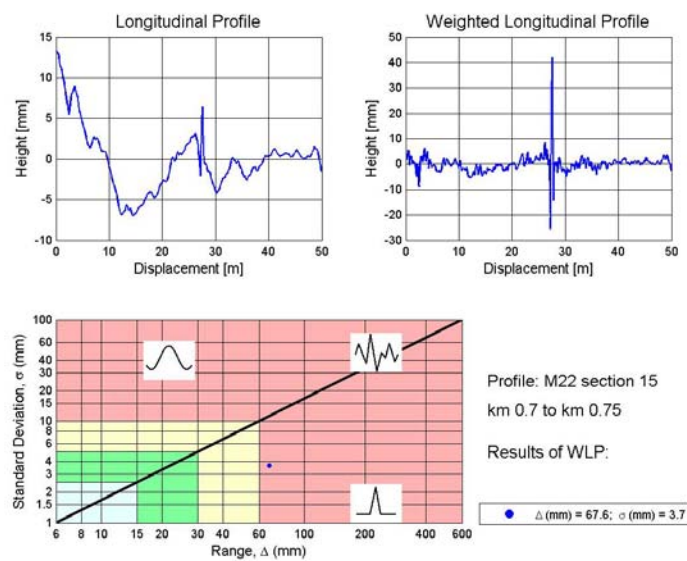


Figure 18. example for a transient of short length (about 0.5 m)

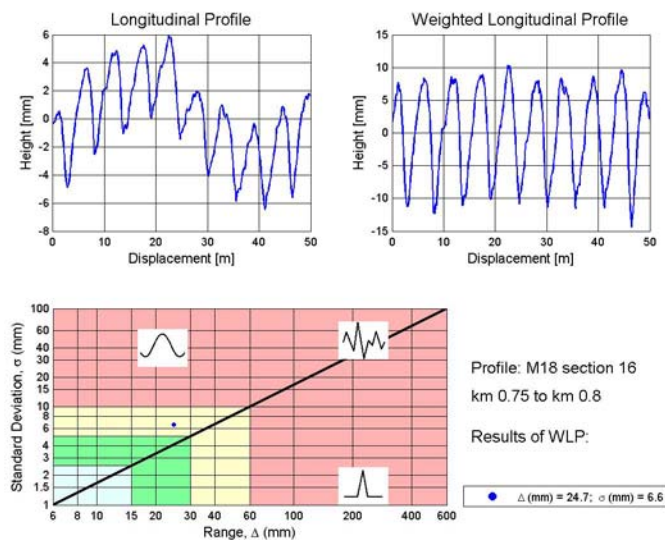


Figure 19. example for a periodicity with a wavelength of about 5 m and an amplitude of 3 mm.

11. Conclusion

The new method presented in this paper – the Weighted Longitudinal Profile (WLP) – proves capable of characterizing all three phenomena of longitudinal evenness: irregular, periodic and transient unevenness. Only two easy understandable indicators are needed: the standard deviation and range of variation.

In comparison with alternative approaches, the method appears to be a promising evaluation concept because it combines the advantages of the response-type methods (implicit evaluation of the shape and size of unevenness with respect to driving dynamics) with those of purely geometrical methods of evaluation (objectivity, without restriction of vibration properties and speed).

12. Bibliography

- Alonso M., Yanguas S., “Analysis of correlations between longitudinal indices in FILTER experiment: Forum of European National Highway Research Laboratories (FEHRL) investigation of longitudinal and transverse evenness of roads experiment”, *Transportation Research Record*, Vol. 1764/2001, p. 243-253
- Andr n P., “Power spectral density approximations of longitudinal road profiles”, *International Journal of Vehicle Design*, Vol. 40, Nos. 1/2/3, 2006
- ASTM E 1489-98 (2003), “Practice for computing Ride Number of roads from longitudinal profile measurements made by an inertial profile measuring device”, ASTM International, 2003
- Boscaino G., Pratic  F. G., Vaiana R., “Texture indicators and surface performance in flexible pavements”, *SURF 2004, PIARC 5-th International Symposium on pavement surface Characteristics – roads and airfields*. Toronto, June 2004.
- Braun H., “Evaluation of pavement unevenness and application of results”, *doctoral thesis*, Technical University of Braunschweig, Germany, 1969 (in German)
- Bruscella B., Rouillard V., Sek M., “Analysis of road surface profiles”, *Journal of Transportation Engineering*, January/February 1999, p. 55-59.
- Buehler B., Klinkhammer S., Maerschalk G., Oertelt S., “Development of a guideline for the measurement and evaluation of the pavement condition, *Forschung Strassenbau und Strassenverkehrstechnik*, Vol. 486, 1986, German Federal Ministry of Transport, Bonn (in German).
- Capuruc , R.A., Hegazy T., Tighe S.L., “Full-car roughness index as summary roughness statistic”, *Transportation Research Board (TRB)*, Vol. 1905, 2005, p. 148-156.
- Delanne Y., Pereira P.A.A., “Advantages and limits of different road roughness profile signal-processing procedures applied in Europe”, *Transportation Research Record*, Vol. 1764/2001, p. 254-259
- Houbolt J.C., “Runway roughness studies in the aeronautical field”, *Transactions of the A.S.C.E.*, Vol. 127 (1962), Part IV, pp.428-447
- Hudson W.R., “Root-mean-square vertical acceleration as a summary roughness statistics”, *ASTM Special Technical Publication, STP No. 884*, T.D. Gillespie and M. Sayers, eds, Philadelphia, Pa.

- ISO 2631-1:1997; “Mechanical vibration and shock – Evaluation of human exposure to whole-body vibration – Part 1: General requirements”, International Organization for Standardization (ISO), 1997
- ISO 8608:1995(E), “Mechanical vibration - Road surface profiles - Reporting of measured data”, International Organization for Standardization (ISO), 1995-09-01.
- Kawamura A., Nakajima S., Shirakawa T., “Lifting scheme theory to detect road surface waveform influencing vehicle vibration”, *Transportation Research Board (TRB)*, Vol. 1949, 2006, p. 164-172
- Loizos A., “A simplified application of fuzzy set theory for the evaluation of pavement roughness”, *Road and Transport Research*, Dec. 2001
- Mitschke M., Braun H., Liesner W., “Permissible amplitudes and wavelengths of periodic unevenness with respect to pavement and cargo loading, safety and vibration perception”, *Forschung Strassenbau und Strassenverkehrstechnik*, No. 486, 1986, German Federal Ministry of Transport, Bonn, Germany, (in German)
- prEN 13036-5, “Surface Characteristics of Road and Air Field Pavements. Test Methods – Part 5: Determination of Longitudinal Unevenness Indices”, European Committee for Standardisation, November 2004
- Rouillard V., Bruscella B., Sek M., “Classification of road surface profiles”, *Journal of Transportation Engineering*, January/February 2000, p. 41-45.
- Praticò F. G., “Nonstrictly-ergodic signals in road roughness analyses: a theoretical and experimental study”, SIIV 2004 – 2nd International Congress, Florence, 27-29 October 2004
- Sayers M.W., “Characteristic Power Spectral Density functions for vertical and roll components of road roughness”, *Symposium on Simulation and Control of Ground Vehicles and Transportation Systems. Proceedings*, ASME, New York, 1986, p. 113-139
- Sayers M.W. *et al.*, “The international road roughness experiment”, *Technical Paper No. 45*, World Bank, Washington D.C., 1986
- Sayers M.W., “Two quarter-car models for defining road roughness: IRI and HRI”, *Transportation Research Record*, 1215, (1989), p. 1-26.
- Sayers M.W., “On the calculation of IRI from longitudinal road profile”, *Transportation Research Record*, 1501, (1996), p. 1-12.
- Shirakawa T., Kawamura A., Nakatsuji T., “Application of the second generation wavelet transform for pavement preventive maintenance”, *Journal of the Eastern Asia Society for Transportation Studies*, Vol. 6, 2005, p. 1113-1122.
- Schniering A., “Supplementary measurements of the irregularities in the longitudinal and transverse profile for elaborating the basis for assessment” Final report on project No. 04.165, Federal Highway Research Institute, Germany, 1998 (in German)
- Ueckermann A., “The Dynamic Evenness Index”, *Forschung Strassenbau und Strassenverkehrstechnik*, No. 839, 2002, German Federal Ministry of Transport, Bonn, Germany, (in German)
- Wei L., Fwa T.F., Zhao Z., “Wavelet analysis and interpretation of road roughness”, *Journal of Transportation Engineering*, February 2005, p. 120-130.
- Wilde W. J., Izevbekhai P.E., Bernard I., Krause M.H., “Comparison of Profile Index and International Roughness Index for pavement smoothness incentive specifications”, *Transportation Research Board (TRB) Annual Meeting Compendium of Papers*, 2007